

Design procedure for seismic retrofit of RC beam-column joint using single diagonal haunch

Alireza Zabihi^a, Hing-Ho Tsang^{*}, Emad F. Gad^b and John L. Wilson^c

Centre for Sustainable Infrastructure, Swinburne University of Technology, Melbourne, Australia

(Received February 20, 2019, Revised April 2, 2019, Accepted April 5, 2019)

Abstract. Exterior beam-column joint is typically the weakest link in a limited-ductile reinforced concrete (RC) frame structure. The use of diagonal haunch element has been considered as a desirable seismic retrofit option for reducing the seismic demand at the joint. Previous research globally has focused on implementing double haunches, while the use of single haunch element as a less-invasive and more architecturally favorable retrofit option has not been investigated. In this paper, the key formulations and a design procedure for the single haunch system for retrofitting RC exterior beam-column joint are developed. An application of the proposed design procedure is then illustrated through a case study.

Keywords: limited-ductile; RC frame; exterior beam-column joint; seismic retrofit; single diagonal haunch

1. Introduction

As reported by the United States Geological Survey, more than 20,000 earthquakes with a magnitude of five or higher occurred worldwide over a 10 year period from 2007 to 2017. The deaths are estimated to be more than 350,000 for this short period of time. This means an average of 100 deaths per day due to this terrifying natural disaster. The majority of the losses was caused by building collapse in the events of earthquakes. Hence, seismic structural engineers can play an important role in mitigating the effects of seismic actions on building structures and hence reducing casualties by providing proper design and/or appropriate retrofitting techniques (e.g. Shiravand *et al.* 2017, Singh *et al.* 2017).

A large number of habitable non-seismically designed RC frame buildings exist all over the world. The poor performance of this kind of buildings has been observed in past earthquake events worldwide (Fig. 1). Previous analytical and experimental studies (Aycardi *et al.* 1994, Beres *et al.* 1996, Calvi *et al.* 2002) proved that non-seismically beam-column joint is the most vulnerable structural element subjected to lateral loads.

This deficiency generally arises from poor detailing in the joint area and consequently lack of capacity design principles in the overall response of the structures (Pampanin *et al.* 2006). To improve the global seismic



Fig. 1 Typical RC beam-column joint failure – an example from 2008 Wenchuan (China) earthquake (photos taken by Hing-Ho Tsang)

behavior of the structure, enhancement of the weakest links is essential which can be achieved by seismic retrofitting. In recent years, various retrofit techniques such as strengthening of joint (e.g. steel jacketing – Fig. 2(a), fiber-reinforced polymer (FRP) composite wrap – Fig. 2(b)) and relocating the plastic hinge away from the joint (e.g. externally clamped double haunch retrofitting system (ECDHRS) – Fig. 2(c), fully fastened double haunch retrofitting system (FFDHRS) – Fig. 2(d)) have been investigated and utilized as practical solutions (Beres *et al.* 1992, Ghobarah & Said 2002, Chen 2006, Genesio 2012, Akbar *et al.* 2018).

Strengthening by steel jacketing or FRP composite and the ECDHRS could be conveniently installed in laboratory tests, but these are challenging to be implemented in practice because of limited accessibility to the joint zone due to the presence of wall and floor slab. Although this limitation has been eliminated by using post-installed mechanical anchors in the FFDHRS (Sharma *et al.* 2014), the use of upper diagonal haunch (located on the floor) still remains as an aesthetic and functional restriction. Hence, the fully fastened single haunch retrofitting system

*Corresponding author, Senior Lecturer, Ph.D.

E-mail: htsang@swin.edu.au

^a Ph.D. Student

E-mail: azabihi@swin.edu.au

^b Professor, Ph.D.

E-mail: egad@swin.edu.au

^c Professor, Ph.D.

E-mail: jwilson@swin.edu.au

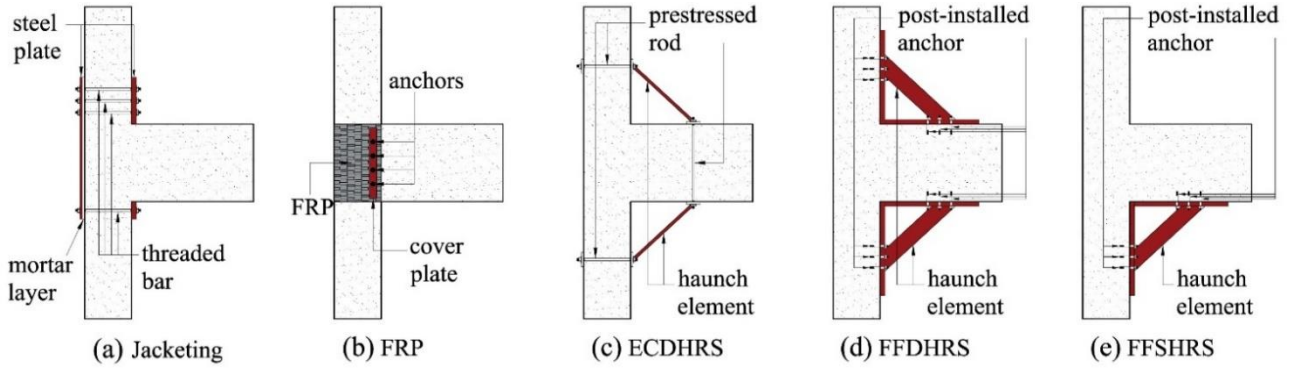


Fig. 2 Schematic diagrams of various retrofit techniques for external RC beam-column joints: (a) Steel jacketing, (b) Fiber-reinforced polymer (FRP) composite wrap, (c) Externally clamped double haunch retrofitting system, (d) Fully fastened double haunch retrofitting system, (e) Fully fastened single haunch retrofitting system

(FFSHRS – Fig. 2(e)) is proposed herein this paper as a preferred alternative.

2. Shear demand at exterior beam-column joint

Based on the applied shear and axial forces, V_c and N_c (as shown in Fig. 3), the shear force and bending moment diagrams of the beam-column joint subassembly for the non-retrofitted system (NRS) and the single haunch retrofitting system (SHRS) are plotted in Figs. 4-5, respectively. For each case, the horizontal shear force at the mid-depth of the joint panel zone, V_{jh} , can be expressed as a function of the applied shear force:

$$V_{jh-NRS} = \left[\frac{H_e}{j_b L_e} \left(\frac{L_n}{2} \right) - 1 \right] V_c \quad (1a)$$

$$V_{jh-SHRS} = \left[\frac{H_e}{j_b L_e} \left(\frac{L_n}{2} - a \beta_{SHRS} \right) - 1 \right] V_c \quad (1b)$$

where H_e = effective height of column between two vertical consecutive inflection points; j_b = lever arm of internal forces in the beam section which can be evaluated through a moment-curvature analysis or approximately assumed as 0.8–0.9 times ($h_b - c$); whereas c is the concrete cover; L_e = beam half length; L_n = net beam span length between column faces; a = horizontal length of the haunch; and β_{SHRS} = shear transferring factor at the beam for SHRS (explained in detail in the next section).

3. Shear transferring factor

The equation for the shear transferring factor, β , can be derived based on the deformation compatibility theory at the haunch-beam and haunch-column connection points (Yu *et al.* 2000, Pampanin *et al.* 2006). Zabihi *et al.* (2018) derived the formulation of β -factor for SHRS by considering both beam and column deformations:

$$\beta_{SHRS} = \frac{N_1 + N_2}{D_1 + D_2 + D_3 + D_4} \tan \alpha \quad (2)$$

where N_1 , N_2 , D_1 , D_2 , D_3 and D_4 can be defined as follows:

$$N_1 = 4ab + 3h_b a + 6Lb + 6h_b L;$$

$$N_2 = \lambda_1 \lambda_2 (4ab + 3h_c b + 6Ha + 6h_c H);$$

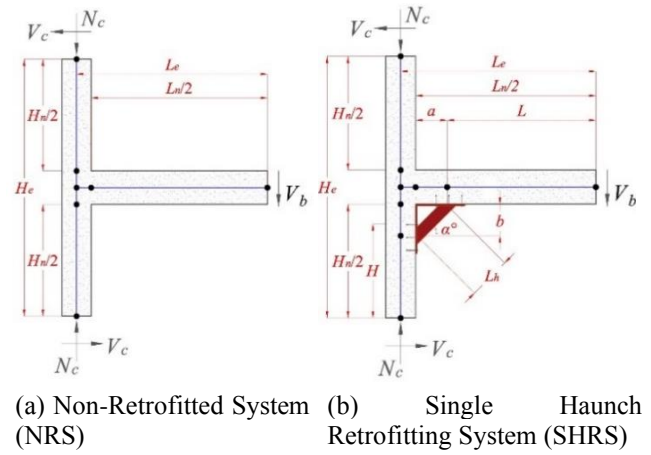


Fig. 3 External actions on exterior beam-column joint

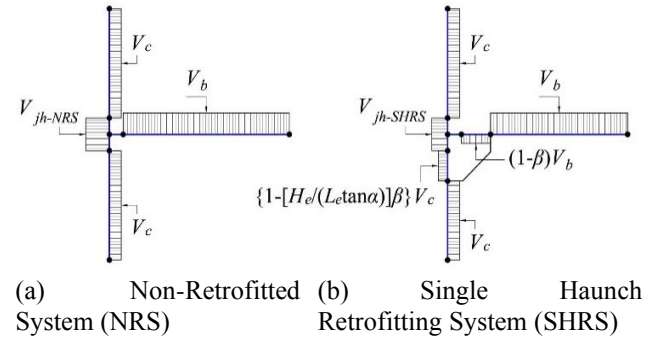


Fig. 4 Shear force diagrams

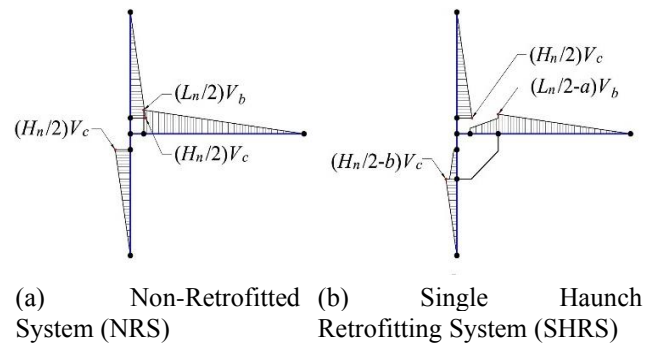


Fig. 5 Bending moment diagrams

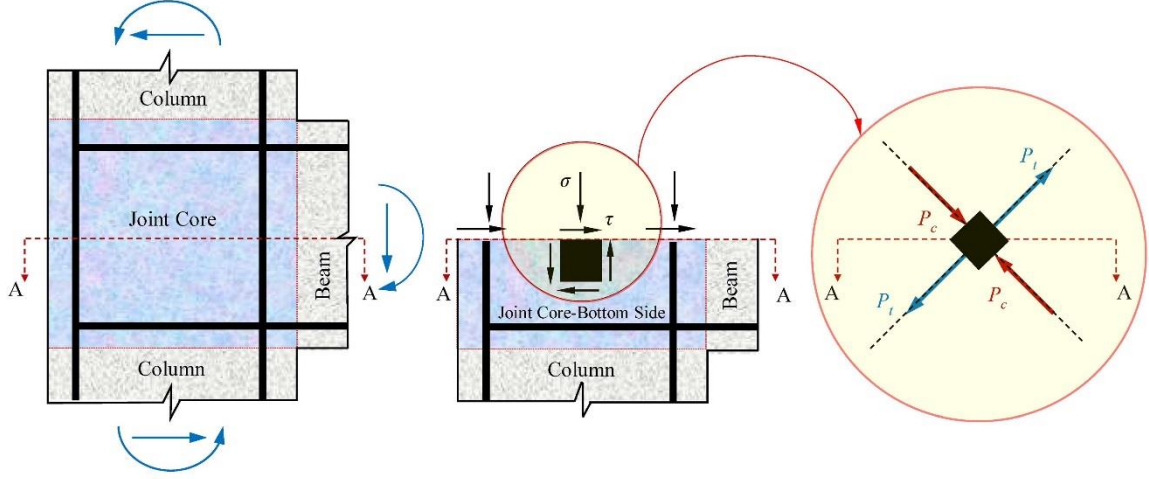


Fig. 6 Stresses in the finite block located in the middle of the joint core (section A-A)

$$\begin{aligned}
 D_1 &= 4ab \tan \alpha + 3h_b a \tan \alpha + 3h_b b + 3h_b^2; \\
 D_2 &= 12E_c I_b / (K_h \cdot a \cos^2 \alpha); \\
 D_3 &= \lambda_1 (4ab \tan \alpha + 6h_c b \tan \alpha + 3h_c^2 \tan^2 \alpha + 12I_c \tan^2 \alpha / A_c); \\
 D_4 &= 12I_b / A_b; \\
 \lambda_1 &= I_b b / (I_c a); \\
 \lambda_2 &= L_e b / (H_e a)
 \end{aligned}$$

in which, b = vertical length of the haunch; h_b = beam section depth; h_c = column section depth; α = angle between the haunch and the beam; E_c = the modulus of elasticity of concrete; I_b = second moment of area of the beam cross section; K_h = haunch stiffness; I_c = second moment of area of the column cross section; A_c = area of the column cross section; A_b = area of the beam cross section; and all other parameters have been explained earlier.

4. Principal tensile stress in exterior beam-column joint

To evaluate the joint shear strength, the principal tensile stress (Fig. 6), p_t , as a function of both joint shear force and column axial load, is a more appropriate damage indicator than joint shear force alone (Priestley 1997, Pampanin *et al.* 2006). The absolute value of the principal tensile stress, p_t , and the principal compressive stress, p_c , at mid-depth of the joint core can be expressed with the use of Mohr's circle theory (Tsonos 1999):

$$p_t = -(\sigma/2) + \sqrt{(\sigma/2)^2 + \tau^2} \quad (3a)$$

$$p_c = +(\sigma/2) + \sqrt{(\sigma/2)^2 + \tau^2} \quad (3b)$$

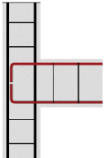
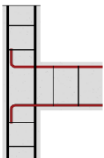
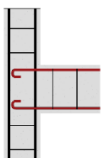
where the average shear stress, τ , and the average normal compressive stress, σ , uniformly distributed over the section A-A (Fig. 6) can be given by:

$$\tau = V_{jh} / (w_j h_j) \quad (4)$$

$$\sigma = (N_c + V_{jv}) / (w_j h_j) \quad (5)$$

in which, w_j and h_j are width and depth of joint core,

Table 1 Limit states of RC beam-column joint based on principal tensile stress

Joint Type		Limit State	
	1st Shear Crack:	$p_t = 0.29\sqrt{f'_c}$	
	Peak Load:	$p_t = 0.42\sqrt{f'_c}$	
	Reference:	Priestley (1997)	
	1st Shear Crack:	$p_t = 0.29\sqrt{f'_c}$	
	Peak Load:	$p_t = 0.29\sqrt{f'_c}$	
	Reference:	Priestley (1997)	
	1st Shear Crack:	$p_t = 0.20\sqrt{f'_c}$	
	Peak Load:	$p_t = 0.20\sqrt{f'_c}$	
	Reference:	Pampanin <i>et al.</i> (2003)	

respectively. The horizontal joint shear force, V_{jh} , can be calculated by using Eqs. (1a)-(1b) and the vertical joint shear force, V_{jv} , can be obtained from force equilibrium in the vertical direction and approximated by (Park & Paulay 1975; Paulay & Park 1984, Tsonos 1999, Sharma *et al.* 2011)

$$V_{jv} = (h_b/h_c)V_{jh} \quad (6)$$

For RC exterior beam-column joint with no transverse reinforcement, the diagonal tension is mainly resisted by concrete. The limiting values of principal tensile stresses for various arrangements of longitudinal bar anchorage are summarized in Table 1. In the joint with 90-degree hooked beam bars (Cases 1 and 2 in Table 1), initial cracking is assumed to occur when $p_t = 0.29\sqrt{f'_c}$. However, bending the longitudinal beam bars 90° into the joint (Case 1 in Table 1) leads to confinement of the concrete diagonal strut in the joint core, and accordingly, enhancement of joint shear strength (Sharma *et al.* 2011). The permissible tensile

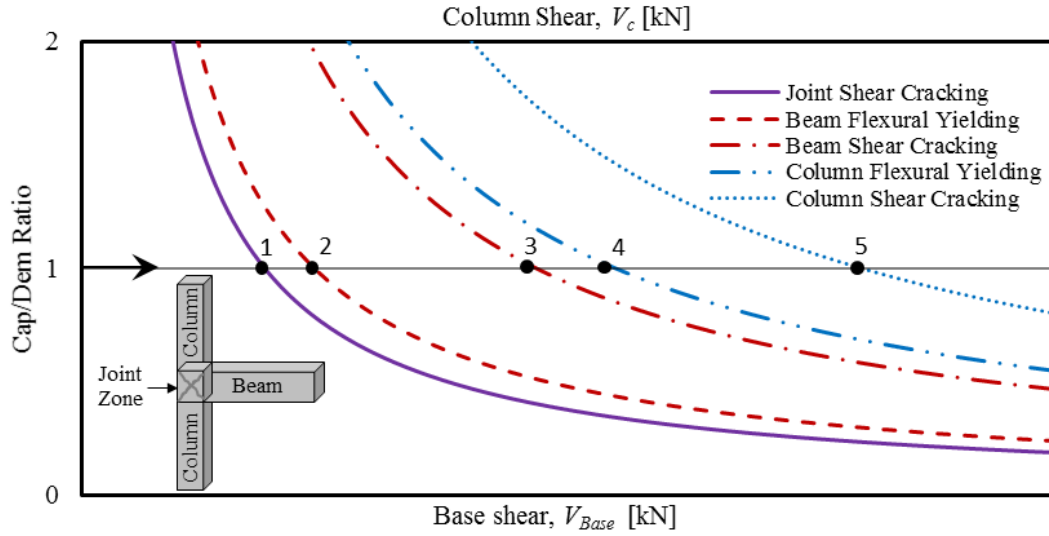


Fig. 7 Conceptual representation of the strength hierarchy assessment for a non-retrofitted limited-ductile RC beam-column joint subassembly

Table 2 The maximum shear and flexural demands imposed on beam and column elements, before and after retrofit

Demand	NRS	SHRS	
$V_{b-max} =$	$\left[\frac{H_e}{L_e}\right] V_c$	$\begin{cases} \left(\frac{H_e}{L_e}\right) V_c & ; \text{ if } \beta_{SHRS} \leq 2 \\ -\left(\frac{H_e}{L_e}\right) (1 - \beta_{SHRS}) V_c; & \text{ if } \beta_{SHRS} > 2 \end{cases}$	(7)
$V_{c-max} =$	V_c	$\begin{cases} V_c & ; \text{ if } \frac{H_e}{L_e \tan \alpha} \beta_{SHRS} \leq 2 \\ -\left[1 - \frac{H_e}{L_e \tan \alpha} \beta_{SHRS}\right] V_c; & \text{ if } \frac{H_e}{L_e \tan \alpha} \beta_{SHRS} > 2 \end{cases}$	(8)
$M_{b-max} =$	$\left[\frac{L_n}{2}\right] \left[\frac{H_e}{L_e}\right] V_c$	$\left[\frac{L_n}{2} - a\right] (H_e/L_e) V_c$	(9)
$M_{c-max} =$	$\left[\frac{H_n}{2}\right] V_c$	$\left[\frac{H_n}{2}\right] V_c$	(10)

Notes: NRS = Non-Retrofitted Subassembly; SHRS = Single Haunch Retrofiting System; V_{b-max} = maximum beam shear demand; M_{b-max} = maximum beam flexural demand; V_{c-max} = maximum column shear demand; M_{c-max} = maximum column flexural demand; and all other parameters have been defined earlier.

strength is assumed to be $p_t = 0.42\sqrt{f'_c}$ beyond which shear hinge is assumed to have formed at the joint (Priestley 1997).

When the beam bars are bent away from the joint (Case 2 in Table 1), it is assumed that the limiting values for principal tensile stress corresponding to the initial shear crack and the peak load are both equal to $0.29\sqrt{f'_c}$ (Priestley 1997). Pampanin *et al.* (2003) proposed a value of $0.20\sqrt{f'_c}$ as the limiting principal tensile stress for smooth bars with end hooks (Case 3 in Table 1). In these two cases, significant and sudden strength reduction is expected to occur after crack formation without any additional source for hardening behavior.

To estimate the allowable column shear force, V_c , corresponding to the joint shear strength limit, the following procedure can be adopted:

- Assume a value of column shear force, V_c
- Calculate horizontal joint shear force, V_{jh} , from Eq. (1)
- Calculate horizontal joint shear stress, τ , from Eq. (4)
- Calculate vertical joint shear force, V_{jv} , from Eq. (6)
- Calculate vertical joint shear stress, σ , from Eq. (5)
- Calculate principal tensile stress, p_t , from Eq. (3a)
- Repeat the procedure above if the obtained value of p_t is not sufficiently close to the limiting value (Table 1).

The use of this procedure is illustrated in the case study example in Section 6. Once the allowable column shear force, V_c , corresponding to the joint shear failure mechanism is obtained, comparison will be made with the values corresponding to other failure mechanisms in order to estimate the most probable failure mode of the subassembly.

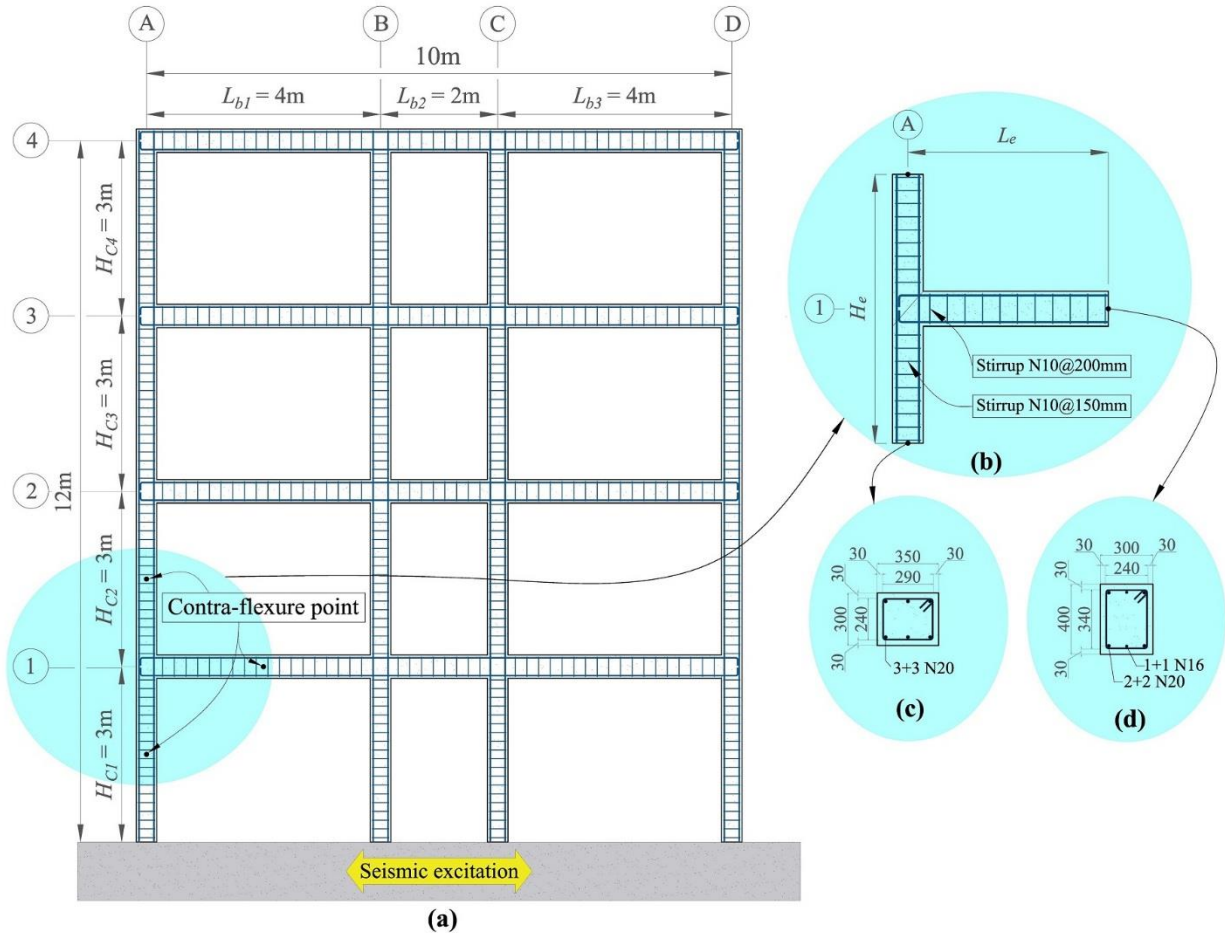


Fig. 8 Geometry of case study model: (a) Full-scale RC moment resisting frame, (b) Exterior beam-column joint, (c) Column section, (d) Beam section

5. Strength hierarchy assessment approach

Each of the constituent elements of the beam-column joint subassembly may fail due to excessive lateral load under different modes, namely, joint shear, beam flexural, beam shear, column flexural, and column shear failure (Genesio 2012). The most probable failure modes can be predicted by the aid of strength hierarchy assessment (Pampanin *et al.* 2004, Hertanto 2005, Chen 2006, Tasligedik *et al.* 2016). In this paper, a capacity-demand ratio diagram, as shown in Fig. 7, is adopted to assess the hierarchy of strength. The capacity-demand ratio is plotted as a function of a demand parameter, such as base shear force, V_{Base} , or column shear force, V_c . The possible failure modes are presented in chronological order of occurrence (e.g. 1 to 5). Failure is assumed to occur when the capacity-demand ratio is smaller than 1.0, and hence, the failure threshold is defined at the point when the ratio equals 1.0.

The estimation of the shear demand and capacity of joint element can be obtained through the procedure discussed in the previous sections. The shear and flexural capacities of beam and column can be determined using traditional ultimate strength methods for reinforced concrete structural design, while the maximum shear and flexural demands imposed on these elements can be obtained based on basic mechanics (refer Figs. 4-5) as summarized in Table 2.

By applying single diagonal haunch, the location and magnitude of maximum shear demand in the beam, as well as the column, can vary depending on the value of shear transferring factor (Chen 2006). Referring to Fig. 4, in cases when the shear transferring factor is less than 2, the maximum shear demand occurs between the endpoint of the element and the point where the haunch meets the element, while it occurs on the other side when the shear transferring factor is larger than 2. Thus, two equations are proposed for the determination of the maximum shear demand at each element (i.e. beam and column) in case of using SHRS. In the next section, the effectiveness of SHRS is demonstrated through a case study.

6. Case study

A full-scale four-story RC moment resisting frame designed based on the requirements in Australia in the 1980's (as shown in Fig. 8(a)) has been considered in this study. No transverse reinforcement was assumed in the joint region in order to be consistent with the old practice. The RC frame is 12 m tall, 10 m wide, and is assumed being located on a very soft soil site (i.e. Class E as defined in AS1170.4-2007) in Melbourne. Properties of the materials used in this case study building are tabulated in Table 3.

Table 3 Material properties of the case study building

Concrete	Reinforcement
$f'_c = 25 \text{ MPa}$	$f_y = 500 \text{ MPa}$
$E_c = 26700 \text{ MPa}$	$f_u = 700 \text{ MPa}$
$\alpha_2 = 0.85$	$E_s = 200 \text{ GPa}$
$\gamma = 0.85$	
$\varepsilon_{cu} = 0.003$	

Notes: f'_c = the characteristic compressive strength of concrete; E_c = the modulus of elasticity of concrete; α_2 = the ratio of equivalent concrete compressive stress developed under flexure to the characteristic compressive strength (f'_c); γ = the ratio, under design bending or design combined bending and compression, of the depth of the assumed rectangular compressive stress block to $k_u d$; whereas d is the effective depth of a cross-section, and k_u is the neutral axis parameter being the ratio, at ultimate strength under any combination of bending and compression, of the depth to the neutral axis from the extreme compressive fiber to d ; ε_{cu} = the ultimate concrete strain; f_y = yield strength of steel reinforcing bar; f_u = ultimate strength of steel reinforcing bar; E_s = the modulus of elasticity of steel.

Due to the absence of shear reinforcement in beam-column joints and thus inadequate shear resistance, brittle failure is expected to occur at the joint zone. The undesirable consequences of this deficiency can be even worse if this failure initiates from one of the joints located at the first floor, which may lead to collapse of the whole structure (refer Fig. 1). Therefore, through this case study, it is first shown that the selected exterior beam-column joint located at the first floor (A1 – Fig. 8(b)) has not been properly designed to withstand the expected earthquake (subsection 6.1) and then a proposed step-by-step design procedure illustrates how the seismic performance of the subassembly can be enhanced by applying a single diagonal haunch (subsection 6.2). At the end of this section, the effect of the length of haunch, L_h , on variation in the strength hierarchy of the beam-column joint subassembly is studied in order to achieve an optimal design.

6.1 Failure assessment of Non-Retrofitted Subassembly (NRS)

To evaluate the performance of the critical beam-column joint subassembly (A1 – Fig. 8(b)) in an event of earthquake, the comparison needs to be made between the design base shear and the allowable base shear corresponding to the strength limit of the most vulnerable element.

The design equivalent static shear force, V_{Base} , at the base of the frame model can be calculated from the following equation in accordance with AS1170.4-2007:

$$V_{Base} = [k_p Z C_h(T_1) S_p / \mu] W_t \quad (11)$$

where k_p = probability factor; Z = earthquake hazard factor; $C_h(T_1)$ = spectral shape factor for the fundamental natural period of the structure; S_p = structural performance factor; μ = structural ductility factor; and W_t = total design seismic

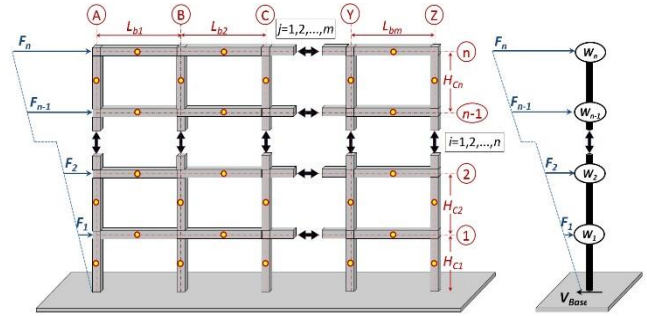


Fig. 9 Schematic view of lateral force distribution

weight of the building which was calculated by assuming 10 kPa gravity loads for all four levels including dead loads and 30% of imposed loads. A single frame model, with half of the bay on each side (4 m in total), is considered in this case study.

Structures are typically categorized into various classes in codes of practice based on their function and the nature of occupancy. In AS1170.4, as in many other codes of practice, the spectral ordinates could be multiplied by an importance factor, or probability factor, k_p , for the design of structures that are considered more important and required to perform better than ordinary structures. According to Table B1.2b in Australia's National Construction Code (NCC) and Table 3.1 in AS1170.4:2007, low-rise residential construction is considered as an ordinary structure with k_p being equal to 1.0. The hazard factor, Z , is the design peak ground acceleration (PGA) (in unit of g) which is 0.08 for Melbourne as the value of the product $k_p Z$ shall not be less than 0.08 for an annual exceedance probability of 1/500 as given in Table 3.3 in AS1170.4:2007 (Lam *et al.* 2016).

The spectral shape factor, $C_h(T_1)$, for the fundamental natural period of this structure ($T_1 = 0.6s$) is 3.68 according to Table 6.4 in AS1170.4:2007, which is also consistent with the proposed value for typical soil sites based on recent research findings (Tsang *et al.* 2017a,b). The structural performance factor, S_p , is taken as 0.77, as given in Table 6.5(A) in AS1170.4:2007, while the structural ductility factor, μ , due to lack of ductility in the joint zone is assumed to be 1.0. By taking the total design seismic weight of the building, W_t , as 1600kN, based on Clause 6.2 in AS1170.4:2007, the design base shear force (with the consideration of over-strength factor S_p) is approximately equal to 360kN (Eq. (11)).

In accordance with Clause 6.3 in AS1170.4-2007, distribution of the lateral forces (Fig. 9), F_i , by considering 100% seismic action in one direction can be obtained by using the following equation:

$$F_i = \frac{W_i h_i^k}{\sum_{j=1}^n (W_j h_j^k)} V_{Base} \quad (12)$$

where W_i = seismic weight of the structure at level i (in kN); h_i = height of level i , above the base of the structure (in m); k = exponent - as given in Clause 6.3 in AS1170.4:2007 - dependent on the fundamental natural period of the structure ($T_1 = 0.6s \rightarrow k = 1.05$); n = number of levels in a structure ($n = 4$). By substituting the obtained

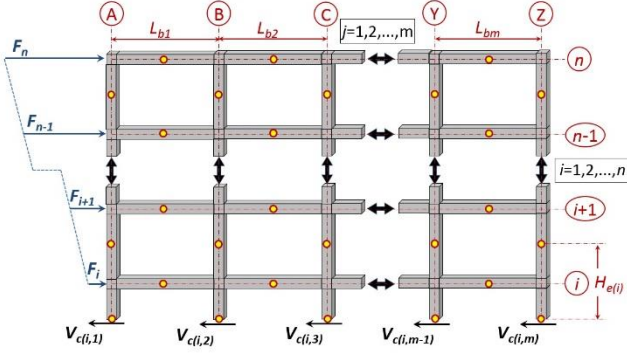


Fig. 10 Column shear force axial load at level (i) based on portal frame method

values in Eq. (12), the lateral force will be 34 kN, 71 kN, 108 kN, and 147 kN at level one, two, three and four, respectively.

The shear force of column j at level i , $V_{c(i,j)}$, can be approximated by utilizing portal frame analysis method (Fig. 10), which is a reasonably accurate method particularly for low-rise buildings. Two assumptions need to be made when this method is used: (1) all contra-flexure points are assumed to be at mid-height of the columns and mid-span of the beams; and (2) the shear force resisted by each column at level i calculated by the following equation:

$$V_{c(i,j)} = \frac{L_{e(i,j)}}{\sum_{j=1}^m L_{bj}} \sum_{k=i}^n F_k \quad (13)$$

By applying Eqs. (12)-(13), a shear force with a magnitude of 72 kN is obtained at the base of the first story exterior column (A1 in Figs. 8(a)-(b)). The lateral load – drift capacity relationship of the first story exterior column can be calculated based on the predictive model proposed by Wibowo *et al.* (2014), Wilson *et al.* (2015) and Raza *et al.* (2018). The peak shear strength, under an axial load ratio of 0.12, is 100 kN, which is higher than the design (72 kN) level. This indicates that the column will respond within the pre-peak range with drift demand less than 1.0%, for nearly the whole range of seismic actions being considered in this study, while the ultimate drift capacity of the column is over 4.0%.

Step-by-step design procedure for seismic retrofit of beam-column joint subassembly with single diagonal haunch is illustrated in Table 4. It is observed that the selected non-retrofitted subassembly (NRS) cannot resist a column shear force of 72 kN due to joint shear failure. Therefore, in order to prevent any types of failure at this subassembly (refer Section 5), a proper seismic retrofitting is required. The following subsection will explain how the seismic performance of the subassembly can be improved by applying the proposed solution and the optimal design of haunch will be determined by varying the length of haunch.

6.2 Design of Single Haunch Retrofitting System (SHRS)

A single diagonal haunch with a length of 600 mm and at an angle of 45 degrees to the beam is proposed to be

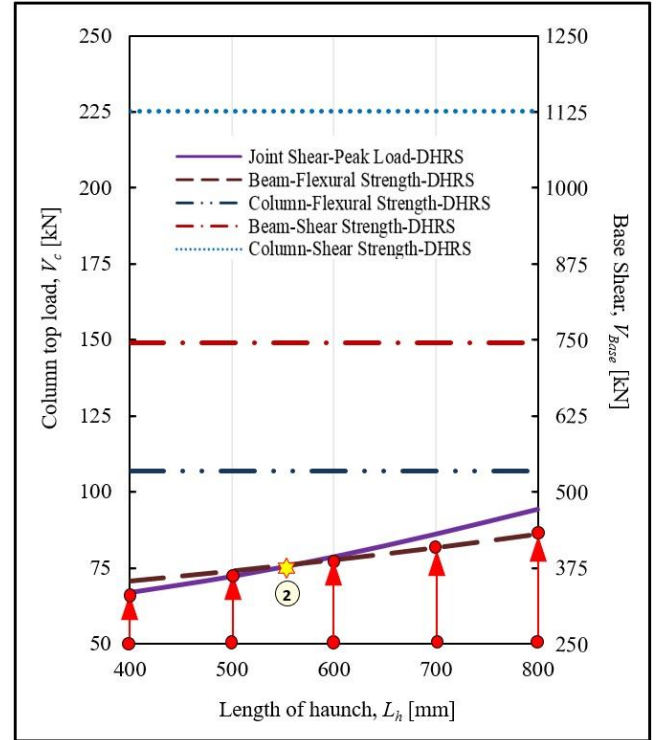


Fig. 11 Assessment of strength hierarchy of the exterior beam-column joint subassembly equipped with a single haunch retrofitting system (SHRS)

implemented on the bottom left beam-column joint subassembly (refer Fig. 3(b)). Through the design procedure proposed in this paper, as detailed in Table 4, applying a 600 mm single diagonal haunch not only strengthens the subassembly against the design base shear level, but also results in favorable yielding mechanism, i.e. beam flexural yielding.

In order to determine an optimum design for SHRS, a parametric study is conducted on the parameter that has the greatest influence on the variation in the strength hierarchy of the beam-column joint subassembly, i.e. length of haunch. The limiting strength due to different failure mechanism is plotted in Fig. 11 as a function of both column shear force, V_c , and base shear force, V_{Base} , against the length of haunch.

As explained earlier, the non-retrofitted subassembly (NRS) is expected to fail due to the formation of undesirable shear hinge at the joint zone at a base shear level of 290 kN (Fig. 12). By applying a single diagonal haunch with 400 mm length and at an angle of 45 degrees to the beam, formation of the shear hinge is shifted from a base shear level of 290 kN to 334 kN. Although the retrofitted joint can resist a stronger earthquake with 15% higher base shear force, it will still fail at the joint zone before reaching the design action level which is considered undesirable from the perspective of capacity design principle.

As shown in Fig. 12 (asterisk 1), the retrofitted joint can resist the design base shear, when the length of the single diagonal haunch is longer than 500 mm. When the single diagonal haunch with a longer length of 565 mm is applied

Table 4 Step-by-step design procedure for retrofitting a non-seismically designed beam-column joint subassembly with a 600mm single diagonal haunch

Geometry of the exterior beam-column joint (A1) subassembly					
Effective height of column	H_e	[mm]	3000		Fig. 3/Fig. 8(b)
Net beam span length between column faces	L_n	[mm]	3700		Fig. 3
Lever arm of internal forces in the beam section	j_b	[mm]	290		Section 2
Beam half length	L_e	[mm]	2000		Fig. 3/Fig. 8(b)
Horizontal length of the haunch	a	[mm]	424.3		Fig. 3(b)
Width of joint core	w_j	[mm]	350		Fig. 8
Depth of joint core	h_j	[mm]	300		Fig. 8
Beam section depth	h_b	[mm]	400		Fig. 8(d)
Column section depth	h_c	[mm]	300		Fig. 8(c)
Joint					
			NRS	SHRS	
Design column shear force	V_c	[kN]	72		Eqs. (11)-(12)-(13)
Beam shear transferring factor	β	--	N/A	1.03	Fig. 4(b)/Eq. (2)
Horizontal joint shear force	V_{jh}	[kN]	617	454	Eq. (1b)
Horizontal joint shear stress	τ	[MPa]	5.88	4.32	Fig. 6/Eq. (4)
Vertical joint shear force	V_{jv}	[kN]	823	605	Eq. (6)
Vertical joint shear stress	σ	[MPa]	10.12	8.05	Fig. 6/Eq. (5)
Principal tensile stress	p_t	[MPa]	2.69	1.88	Fig. 6/Eq. (3a)
--	$p_t / \sqrt{f_c'}$	--	0.54	0.38	Table. 3
Anchorage type			Case 1		Figs. 8(a)-(b)
Shear strength of joint as a function of $p_t / \sqrt{f_c'}$			0.42		Table. 1
Capacity-demand ratio			0.78<1.0	1.12>1.0	Section 5/Fig. 7
Failure occurred?			Yes	No	
Beam					
			NRS	SHRS	
Design column shear force			72		Eqs. (11)-(12)-(13)
Maximum beam shear demand	V_{b-max}	[kN]	108	108	Eq. (7)
Shear strength of beam	V_b	[kN]	224		Ultimate strength method
Capacity-demand ratio			2.07>1.0	2.07>1.0	Section 5/Fig. 7
Failure occurred?			No	No	
Maximum beam flexural demand	M_{b-max}	[kN.m]	200	154	Eq. (9)
Flexural strength of beam	M_b	[kN.m]	166		Ultimate strength method
Capacity-demand ratio			0.83<1.0	1.08>1.0	Section 5/Fig. 7
Failure occurred?			Yes	No	
Column					
			NRS	SHRS	
Design column shear force			72		Eqs. (11)-(12)-(13)
Maximum column shear demand			72	72	Eq. (8)
Shear strength of column			225		Ultimate strength method
Capacity-demand ratio			3.13>1.0	3.13>1.0	Section 5/Fig. 7
Failure occurred?			No	No	
Maximum column flexural demand	M_{c-max}	[kN.m]	94	94	Eq. (10)
Flexural strength of column	M_c	[kN.m]	139		Ultimate strength method
Capacity-demand ratio			1.49>1.0	1.49>1.0	Section 5/Fig. 7
Failure occurred?			No	No	
Summary					
NRS	(Capacity/Demand) _{NRS} : Joint Shear < Beam Flexural < 1.0 < Column Flexural < Beam Shear < Column Shear				
	↓				
	Failure occurred due to formation of undesirable shear hinge at the joint panel zone				
	↓				
	Retrofitting required				
	↓				
SHRS	(Capacity/Demand) _{SHRS} : 1.0 < Beam Flexural < Joint Shear < Column Flexural < Beam Shear < Column Shear				
	↓				
	All capacity-demand ratios are bigger than 1.0 (Refer to Section 5)				
	↓				
	Retrofit works				

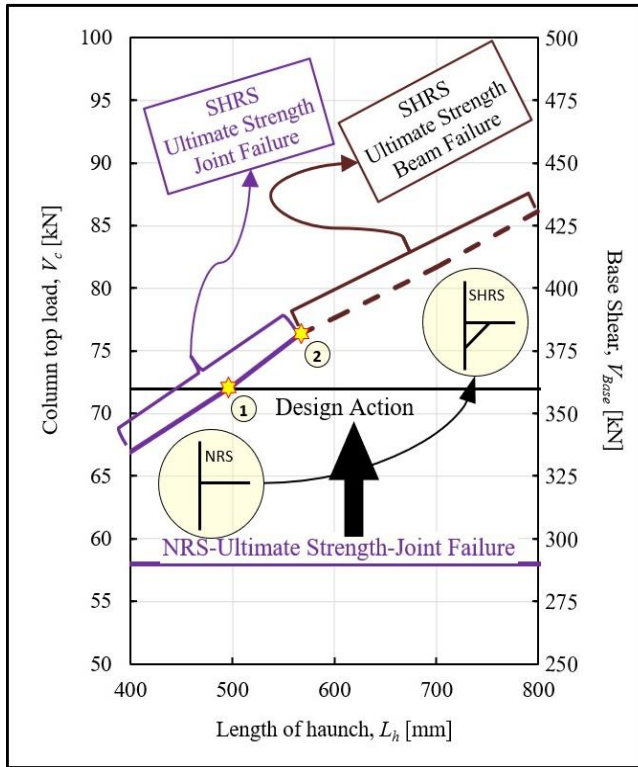


Fig. 12 Summary of the ultimate strength and failure mode of the exterior beam-column joint subassembly before and after retrofit

Table 5 Failure threshold and capacity enhancement

	L_h	V_{Base}	Enhancement	Failure Mode
NRS	--	290 kN	--	Joint Shear
	400mm	334 kN	15%	Joint Shear
	500mm	361 kN	24%	Joint Shear
SHRS	600mm	388 kN	34%	Beam Flexural
	700mm	408 kN	41%	Beam Flexural
	800mm	431 kN	49%	Beam Flexural

Notes: L_h = Length of haunch, V_{Base} = Base shear force.

to the beam-column joint subassembly, both joint shear hinging and beam plastic hinging may occur at a higher base shear level of 380 kN (asterisk 2 in Figs. 11 and 12).

This level can be defined as the balanced scenario, while a longer haunch results in favorable yielding mechanism, i.e. beam flexural yielding, as well as a slightly higher capacity enhancement. In other words, in order to achieve both benefits of single haunch retrofitting system (i.e. resisting against the design action and changing the failure mechanism) at this particular beam-column joint subassembly, the length of haunch has to be longer than 565 mm. Implementing a single diagonal haunch with 500 mm, 700 mm, and 800 mm length and at an angle of 45 degrees will shift the failure threshold to the base shear level of 361 kN, 408 kN, and 431 kN, respectively. The key results, which can be obtained through the proposed design procedure as explained in Table 4, are summarized in Table 5.

7. Summary and conclusions

This paper presents the key formulation and a step-by-step procedure for the design of a single diagonal haunch system, which is a less-invasive and architecturally more favorable seismic retrofitting technique for RC beam-column joint. The shear demand at the joint with and without the single haunch element (Section 2), the shear transferring factor (β) as the pivotal parameter in the design of the haunch retrofitting system (Section 3), the shear capacity at the joint (Section 4), and the strength hierarchy assessment approach (Section 5) have been presented. In Section 6, the seismic performance of the critical exterior beam-column joint subassembly of a full-scale four-story RC moment resisting frame before and after retrofit has been investigated and the proposed design procedure has been illustrated and explained in details through a case study. It is shown that the seismic behavior of a poorly detailed exterior beam-column joint can be improved by the installation of a single diagonal haunch. Furthermore, the effect of the length of haunch on the variation in the strength hierarchy has been studied in order to achieve an optimal design. The results presented in this paper can provide insights for the design and optimization of the single haunch retrofitting system (SHRS).

Acknowledgments

The authors acknowledge the financial supports from the Bushfire and Natural Hazards Cooperative Research Centre of the Australian Government.

References

- Akbar, J., Ahmad, N., Alam, B. and Ashraf, M. (2018), "Seismic performance of RC frames retrofitted with haunch technique", *Struct. Eng. Mech.*, **67**(1), 1-8. <https://doi.org/10.12989/sem.2018.67.1.001>.
- Australian Building Codes Board (2016), *National Construction Code of Australia – Class 2 and 9 Buildings – Volume One*, Canberra, ACT, Australia.
- Aycardi, L.E., Mander, J.B. and Reinhorn, A.M. (1994), "Seismic resistance of reinforced concrete frame structures designed only for gravity loads", *ACI Struct. J.*, **91**(5), 552-563.
- Beres, A., El-Borgi, S., White, R.N. and Gergely, P. (1992), "Experimental results of repaired and retrofitted beam-column joint tests in lightly reinforced concrete frame buildings", NCEER-92-0025; National Center for Earthquake Engineering Research, Taipei, Taiwan. <http://hdl.handle.net/10477/610>.
- Beres, A., Pessiki, S.P., White, R.N. and Gergely, P. (1996), "Implications of experiments on the seismic behavior of gravity load designed RC beam-to-column connections", *Earthq. Spectra*, **12**(2), 185-198. <https://doi.org/10.1193/1.1585876>.
- Calvi, G.M., Magenes, G. and Pampanin, S. (2002), "Relevance of beam-column joint damage and collapse in RC frame assessment", *J. Earthq. Eng.*, **6**(S1), 75-100.
- Chen, T. (2006), "Retrofit strategy of non-seismically designed frame systems based on a metallic haunch system", M.Sc. Dissertation, University of Canterbury, Christchurch.
- Genesio, G. (2012), "Seismic assessment of RC exterior beam-column joints and retrofit with haunches using post-installed anchors", Ph.D. Dissertation, University of Stuttgart, Stuttgart.
- Ghobarah, A. and Said, A. (2002), "Shear strengthening of beam-

- column joints", *Eng. Struct.*, **24**(7), 881-888. [https://doi.org/10.1016/S0141-0296\(02\)00026-3](https://doi.org/10.1016/S0141-0296(02)00026-3).
- Hertanto, E. (2005), "Seismic assessment of pre-1970s reinforced concrete structure", M.Sc. Dissertation, University of Canterbury, Christchurch.
- Lam, N.T.K., Tsang, H.H., Lumantarna, E. and Wilson, J.L. (2016), "Minimum loading requirements for areas of low seismicity", *Earthq. Struct.*, **11**(4), 539-561. <https://doi.org/10.12989/eas.2016.11.4.539>.
- Pampanin, S., Magenes, G. and Carr, A. (2003), "Modelling of shear hinge mechanism in poorly detailed RC beam-column joints", *Proceedings of the FIB 2003 Symposium*, Athens. <http://hdl.handle.net/10092/194>.
- Pampanin, S., Bolognini, D., Pavese, A., Magenes, G. and Calvi, G.M. (2004), "Multi-level seismic rehabilitation of existing frame systems and subassemblies using FRP composites", *Proceedings of the 2nd International Conference on FRP Composites in Civil Engineering*, Adelaide, Australia, December.
- Pampanin, S., Christopoulos, C. and Chen, T. (2006), "Development and validation of a metallic haunch seismic retrofit solution for existing under-designed RC frame buildings", *Earthq. Eng. Struct. Dynam.*, **35**(14), 1739-1766. <https://doi.org/10.1002/eqe.600>.
- Park, R. and Paulay, T. (1975), *Reinforced Concrete Struct.*, John Wiley and Sons, USA.
- Paulay, T. and Park, R. (1984), "Joints in reinforced concrete frames designed for earthquake resistance", *Report prepared for the U.S.-N.Z.-Japan Seminar*, Christchurch, July.
- Priestley, M.J.N. (1997), "Displacement-based seismic assessment of reinforced concrete buildings", *J. Earthq. Eng.*, **1**(1), 157-192.
- Raza, S., Tsang, H.H. and Wilson, J.L. (2018), "Unified models for post-peak failure drifts of normal and high-strength RC columns", *Mag. Concrete Res.*, **70**(21), 1081-1101. <https://doi.org/10.1680/jmacr.17.00375>.
- Sharma, A., Reddy, G.R., Eligehausen, R., Genesio, G. and Pampanin, S. (2014), "Seismic response of reinforced concrete frames with haunch retrofit solution", *ACI Struct. J.*, **111**(3), 673-684.
- Sharma, A., Eligehausen, R. and Reddy, G.R. (2011), "A new model to simulate joint shear behavior of poorly detailed beam-column connections in RC structures under seismic loads, Part I: Exterior joints", *Eng. Struct.*, **33**(3), 1034-1051. <https://doi.org/10.1016/j.engstruct.2010.12.026>.
- Shiravand, M.R., Nejad, A.K. and Bayanifar, M.H. (2017), "Seismic response of RC structures rehabilitated with SMA under near-field earthquakes", *Struct. Eng. Mech.*, **63**(4), 497-507. <https://doi.org/10.12989/sem.2017.63.4.497>.
- Singh, B., Chidambaram, R.S., Sharma, S. and Kwatra, N. (2017), "Behavior of FRP strengthened RC brick in-filled frames subjected to cyclic loading", *Struct. Eng. Mech.*, **64**(5), 557-566. <https://doi.org/10.12989/sem.2017.64.5.557>.
- Standards Australia (2007), *AS 1170.4-2007*, Structural Design Actions; Part 4: Earthquake Actions, Australian Standard, Sydney, Australia.
- Tasligedik, A.S., Akguzel U., Kam W.Y. and Pampanin, S. (2018), "Strength hierarchy at reinforced concrete beam-column joints and global capacity strength hierarchy at reinforced concrete beam-column joints and global capacity", *J. Earthq. Eng.*, **22**(3), 454-487. <https://doi.org/10.1080/13632469.2016.1233916>.
- The United States Geological Survey (2018), Earthquake Statistics, USA. <https://earthquake.usgs.gov/>
- Tsang, H.H., Wilson, J.L., Lam, N.T.K. and Su, R.K.L. (2017), "A design spectrum model for flexible soil sites in regions of low-to-moderate seismicity", *Soil Dynam. Earthq. Eng.*, **92**, 36-45. <https://doi.org/10.1016/j.soildyn.2016.09.035>.
- Tsang H.H., Wilson, J.L. and Lam, N.T.K. (2017), "A refined design spectrum model for regions of lower seismicity", *Australian J. Struct. Eng.*, **18**(1), 3-10. <https://doi.org/10.1080/13287982.2017.1297529>.
- Tsonos, A.G. (1999), "Lateral load response of strengthened reinforced concrete beam to column joints", *ACI Struct. J.*, **96**, 46-56.
- Wibowo, A., Wilson, J.L., Lam, N. TK. and Gad, E.F. (2014), "Drift performance of lightly reinforced concrete columns", *Eng. Struct.*, **59**, 522-535. <https://doi.org/10.1016/j.engstruct.2013.11.016>.
- Wilson, J.L., Wibowo, A., Lam, N.T.K. and Gad, E.F. (2015), "Drift behaviour of lightly reinforced concrete columns and structural walls for seismic design applications", *Australian J. Struct. Eng.*, **16**(1), 62-74.
- Yu, Q. "Kent", Uang, C. and Gross, J. (2000), "Seismic rehabilitation design of steel moment connection", *ASCE J. Struct. Eng.*, **126**(1), 69-78. [https://doi.org/10.1061/\(ASCE\)0733-9445\(2000\)126:1\(69\)](https://doi.org/10.1061/(ASCE)0733-9445(2000)126:1(69)).
- Zabihi, A., Tsang, H.H., Gad, E.F. and Wilson, J.L. (2018), "Seismic retrofit of exterior RC beam-column joint using diagonal haunch", *Eng. Struct.*, **174**, 753-767. <https://doi.org/10.1016/j.engstruct.2018.07.100>.

CC